Biochimica et Biophysica Acta 1844 (2014) 2127–2134

Contents lists available at ScienceDirect

Biochimica et Biophysica Acta

journal homepage: www.elsevier.com/locate/bbapap

Solution conditions define morphological homogeneity of α-synuclein fibrils

Arshdeep Sidhu [a], Ine Segers-Nolten [a], Vinod Subramaniam [a,b,c,*]

[a] Nanobiophysics, MESA + Institute for Nanotechnology, University of Twente, Enschede, The Netherlands
[b] MIRA Institute for Biomedical Technology and Technical Medicine, University of Twente, Enschede, The Netherlands
[c] FOM Institute AMOLF, Amsterdam, The Netherlands

ARTICLE INFO

Article history:
Received 14 July 2014
Received in revised form 4 September 2014
Accepted 5 September 2014
Available online 16 September 2014

Keywords:
α-Synuclein
Morphology
Fibrillization
Periodicity
Homogeneous

ABSTRACT

The intrinsically disordered human α-synuclein (αSyn) protein exhibits considerable heterogeneity in *in vitro* fibrillization reactions. Using atomic force microscopy (AFM) we show that depending on the solvent conditions, A140C mutant and wild-type αSyn can be directed to reproducibly form homogeneous populations of fibrils exhibiting regular periodicity. Results from Thioflavin-T fluorescence assays, determination of residual monomer concentrations and native polyacrylamide gel electrophoresis reveal that solvent conditions including EDTA facilitate incorporation of a larger fraction of monomers into fibrils. The fibrils formed in 10 mM Tris–HCl, 10 mM NaCl and 0.1 mM EDTA at pH 7.4 display a narrow distribution of periodicities with an average value of 102 ± 6 nm for the A140C mutant and 107 ± 9 nm for wt αSyn. The ability to produce a homogeneous fibril population can be instrumental in understanding the detailed structural features of fibrils and the fibril assembly process. Moreover, the availability of morphologically well-defined fibrils will enhance the potential for use of amyloids as biological nanomaterials.

1. Introduction

Self-assembled protein structures have been associated with several age related degenerative diseases like Parkinson's disease (PD), Alzheimer's disease (AD) and diabetes [1–3]. However, the propensity of a large number of proteins to form amyloid fibrils *in vitro* irrespective of their primary sequence has resulted in an extension of amyloid science from not only understanding mechanisms involved in fibrillization, diagnostics [4,5] and potential therapeutics [6–8] but also to studying their mechano-physical properties and designing functionalized fibrils *via* biochemical modifications for custom applications [9,10]. In the past decade, functionalities of amyloids have been extensively explored for use as nanomaterials. Fibrillar amyloids have been shown to be promising candidates as bio-templates for tissue engineering and bio-mineralization [11] and as metal or polyelectrolyte conjugated nanowires [12–15]. However, at present the applicability of the fibrils as bio-nanomaterials is considerably limited by the inherent heterogeneity in the *in vitro* fibrillization.

Fibrillization is a nucleation dependent polymerization process, in which nucleation is usually induced *de novo* by protein monomers but can also be circumvented by including pre-formed fibrils (seeded aggregation) [16,17]. The early phase of aggregation is suggested to be a complex molecular mix, where at different time points, alternative competing reaction pathways like fragmentation or surface catalyzed nucleation (secondary nucleation) may be favored [18–22]. The plateau phase of the aggregation reaction is an assortment of monomers, oligomers and fibrils with the morphology of the mature fibrils exhibiting appreciable heterogeneity [21,23–25]. Morphological heterogeneity or structural polymorphism can be inherent as seen with proteins like Amyloid β [26], αSyn [21,27,28], Ig light chains [29], ovalbumin [30], β-lactoglobulin and lysozyme [31], which form morphologically distinct assemblies under the same solvent conditions. Also, specific solvent conditions may favor certain morphology. Numerous reports have shown the critical role of solvent conditions like ionic strength, pH, temperature, inclusion of metal ions, and other small molecules on the aggregation kinetics and morphology of the fibrils [6–8,32–41]. In general, factors favoring faster fibrillization like higher salt, higher temperature and low pH are shown to result in more heterogeneous aggregations [42].

Features like height, periodicity and length are typically used to describe the morphology of amyloid fibrils. Of these, height and periodicity are shown to be dependent on the number of protofilaments in the fibrils and can be determined accurately by AFM at single fibril level in a direct and model free regime [34,35,37,38,40,43]. Length on the other

Abbreviations: αSyn, α-synuclein; AFM, Atomic Force Microscopy; A140C αSyn, substitution mutant of αSyn with residue 140 mutated from alanine to cysteine; EDTA, ethylenediaminetetraacetic acid; TCEP, tris(2-carboxyethyl)phosphine hydrochloride; DTT, dithiothreitol; ThT, thioflavin-T; DTNB, [5,5′-dithiobis-(2-nitrobenzoic acid)]

* Corresponding author at: FOM Institute AMOLF, Science Park 104, 1098 XG Amsterdam, The Netherlands. Tel.: +31 20 7547100.
E-mail address: subramaniam@amolf.nl (V. Subramaniam).

http://dx.doi.org/10.1016/j.bbapap.2014.09.007
1570-9639/

hand is critically affected by agitation during the aggregation reaction and stochastic shear forces inherent with handling, both of which favor fragmentation [33,39]. Moreover, length analysis of the fibrils deposited on the mica surface is reported to have adsorption (during sample preparation) and detection (during analysis) bias towards shorter or longer fibrils [36,44].

In the present study we use αSyn as a model protein and report the formation of mature αSyn fibrils with homogeneous morphology. αSyn is a 140 amino acid predominantly neuronal protein implicated in the pathogenesis of Parkinson's disease and other synucleopathies [1,2]. We systematically imaged a large number of single fibrils at high resolution (3.3 nm/pixel) with AFM and quantified the fibril morphology with respect to their height and periodicity. αSyn, like other amyloidogenic proteins assembles into fibrillar species *in vitro* under a range of solvent conditions and displays highly polymorphic mature fibrils [21,24,33,42,45]. Furthermore, aggregation kinetics of αSyn (wt and mutants) is known to be highly irreproducible and recently a number of studies have reported on new approaches to improve reproducibility of *in vitro* fibrillization assays [32,46,47].

In our study, the mutant carrying a cysteine at position 140 instead of an alanine (A140C) and wild type (wt) protein were used. Given the relative ease of functionalization of cysteine through the –SH group, replacement of alanine by cysteine facilitates biochemical modifications and makes this mutant an important sequence polymorph for functionalization studies. Also being at the carboxyl terminus, the residue is exposed to the solvent in the mature fibril and as such is less likely to interfere in the process of fibrillization [43,48,49]. Incubation of A140C αSyn in solvent conditions with 10 mM NaCl including 2 mM DTT (dithiothreitol) and 0.1 mM EDTA (ethylenediaminetetraacetic acid) at pH 7.4 for fibrillization followed by AFM imaging and subsequent image analysis revealed the formation of a homogeneous pool of fibrils with an average periodicity of 102 ± 6 nm and height of 6.4 ± 0.4 nm. EDTA was included in the reaction to enhance the half-life of DTT (used to prevent dimerization of A140C by intermolecular disulfide bond formation). Similar experiments using wt αSyn also showed that inclusion of EDTA influences the fibrillization reaction leading to formation of fibrils exhibiting uniform periodicities with an average value of 107 ± 9 nm and fibril height of 6.9 ± 0.6 nm. Together, these results show that the inclusion of EDTA in the given fibrillization reaction conditions induces the formation of fibrils with uniform heights and periodicities.

2. Materials and methods

2.1. Expression and purification of αSyn

wt and A140C αSyn were used in the present study. *Escherichia coli* BL21(DE3) cells transformed with the pT7-7 plasmid carrying the wt αSyn gene were cultured in 1 liter of LB medium with 100 μg/ml ampicillin. At an OD of 0.6–0.7 the T-7 promoter was induced by 1 mM IPTG for 4 hours. Cells were harvested by centrifugation at 6000 × *g* for 10 min. The cell pellet was resuspended in 1/10th of the culture volume in 10 mM Tris–HCl, pH 8.0, 1 mM EDTA and 1 mM PMSF, and stirred for 1 hour at 4 °C. Cells were lysed by sonication for 2 min. Cellular debris was removed by centrifugation at 10,000 × *g* for 20 min at 4 °C. Nucleic acids were removed from the lysate by adding 1% (w/v) of streptomycin sulfate and stirring for 15 min at 4 °C, followed by centrifugation at 13,500 × *g* for 30 min at 4 °C. αSyn was salted-out from the solution by slow addition of 0.295 g/ml of ammonium sulfate and mild stirring for 1 hour at 4 °C. Precipitated protein was collected by centrifugation at 13,500 × *g* for 30 min at 4 °C. The ammonium sulfate pellet was gently resuspended in 1/20th of the culture volume in 10 mM Tris–HCl, pH 7.4 and filtered through a 0.22 μm filter. The solution was loaded onto a 6 ml ResourceQ column using an Åkta Purifier system (GE Healthcare). αSyn was eluted using a linear gradient of NaCl (0–500 mM) in 10 mM Tris–HCl, pH 7.4 at a flow-rate of 3 ml/min over 20 column volumes and 1 ml fractions were collected. Fractions were checked for αSyn using SDS–PAGE and pooled. The pooled sample was concentrated (Vivaspin-20, 10 kDa; GE Healthcare) to a volume of <2.5 ml. The sample was desalted with a PD-10 column (GE Healthcare) using 10 mM Tris–HCl pH 7.4. The volume was adjusted with Tris–HCl, pH 7.4 to a concentration of 250 μM, and divided in aliquots of 0.5 ml and stored at −80 °C. The A140C mutant construct was generated by site directed mutagenesis using a QuikChange II Site-Directed Mutagenesis Kit (Stratagene). A140C protein was expressed and purified according to the same protocol as wt αSyn, with additional inclusion of 1 mM DTT in all buffers.

2.2. Fibrillization reaction

Two hundred fifty micromolar monomeric stocks of wt and A140C mutant αSyn frozen at −80 °C were thawed and filtered through 0.02 μm, 10 mm Anotop10 Whatman syringe filters. Aggregation reactions were set up with 100 μM A140C αSyn, 10 mM Tris–HCl, 1 or 10 mM NaCl, (+/-) 0.1 mM EDTA, 2 mM fresh DTT at pH 7.4 and with 100 μM wt αSyn, 10 mM Tris–HCl, 1 or 10 mM NaCl, (+/-) 0.1 mM EDTA at pH 7.4. All reactions were prepared in triplicate with volumes of 400 μl each in 2 ml Lo-Bind round bottom Eppendorf centrifuge tubes and were incubated at 37 °C with 500 rpm orbital shaking in an Eppendorf Thermo-mixer comfort. Fibrillization using Tris(2-carboxyethyl)phosphine hydrochloride (TCEP-Fluka BioChemika) was done in a similar manner as with DTT with minor differences. The protein aliquots from –80 °C were desalted using a Zeba spin desalting column (7 k MWCO; Pierce Biotechnology) to remove residual DTT and 100 μM A140C αSyn solutions were prepared in 10 mM Tris–HCl, 10 mM NaCl, 2 mM TCEP (final concentrations) at pH 7.4.

2.3. Thioflavin-T assay

Progress of fibrillization was followed by a Thioflavin-T (ThT) fluorescence assay. A stock solution of 1 mM ThT was prepared in 50 mM glycine–NaOH buffer, pH 8.2 and filtered through a 0.22 μm syringe filter. At each time point (every 24 hours), 5 μl aliquots of sample were drawn and diluted in 2 ml of 5 μM ThT working solution diluted in glycine–NaOH buffer, pH 8.2. Fluorescence intensity was measured in triplicate on a Cary Eclipse fluorescence spectrophotometer (Varian Inc., Palo Alto, CA, USA), with excitation at 457 nm and emission detection from 475 to 600 nm using slit widths of 10 nm. ThT curves were prepared by plotting the emission intensity readings at 485 nm *versus* aggregation time; triplicate values were averaged and blank subtracted.

2.4. Residual monomer concentration (RMC)

The amount of monomers left in the aggregation reaction after attaining the plateau phase in a ThT assay was determined by centrifugation of 200 μl aliquots of aggregation reactions at 21,000 × *g* for 1 hour in an IEC Micromax microcentrifuge (Thermo Fisher Scientific Holding B.V., Breda, The Netherlands). The supernatant recovered from the centrifuged samples was filtered through 0.02 μm, 10 mm Anotop10 Whatman syringe filters and the absorbance was measured at 280 nm and 330 nm in a Shimadzu UV-2401 PC spectrophotometer (Shimadzu Benelux B.V., 's-Hertogenbosch, The Netherlands). The absorption values at 280 nm were corrected for scattering contributions before calculating the residual monomer concentration [50].

2.5. Atomic force microscopy — fibril morphology analysis

AFM samples were prepared by adsorbing 20 μl of fibril sample, 5 to 10 times diluted in 10 mM Tris–HCl, 10 mM NaCl at pH 7.4 on freshly cleaved mica (Muscovite mica, V-1 quality, EMS) for 4 min, followed by 2 gentle washes with 100 μl of fresh Milli-Q water and drying in a

gentle stream of nitrogen gas. AFM images were acquired on a Bioscope Catalyst (Bruker, Santa Barbara, CA, USA) in soft tapping mode in air using a silicon probe, NSC36 tip B with force constant of 1.75 N/m (MikroMasch, Tallin, Estonia). All images were captured with a resolution of 512 samples/line with a scan rate of 0.5 Hz and a scan size of 1.7 × 1.7 μm. For each solvent condition about 100 non-overlapping fibrils more than 1 μm in length were qualitatively analyzed by scanning probe image processor — 6.02 (Image Meterology A/S, Hørsholm, Denmark) software; for quantitative analysis of height (h) and periodicity (p) a custom written Matlab script using DIPimage toolbox (version 2.3, TU Delft, Delft, The Netherlands) was used. The script is based on quantitative analysis of AFM images as described elsewhere [27].

2.6. DTNB assay

DTNB [5,5′-dithiobis-(2-nitrobenzoic acid)] assay was carried out to quantify the amount of active DTT (free thiols) in aggregation reactions with and without EDTA. Ten millimolar DTNB stock solution was prepared in 0.1 M sodium phosphate buffer, pH 8.0 and filtered through a 0.22 μm syringe filter. For each time point reading, a standard curve for DTT over a concentration range of 5 to 50 μM was prepared with a working concentration of 1 mM DTNB. Five microliter aggregation aliquots were drawn at each time point and added to 1 ml of 1 mM DTNB solution in 0.1 mM sodium phosphate buffer pH 8.0 and absorbance was measured at 412 nm on a Shimadzu UV-2401 PC spectrophotometer (Shimadzu Benelux B.V., 's-Hertogenbosch, The Netherlands). The concentration of the free thiols in aggregation reactions was calculated using A_{412nm} absorbance readings and the slope of the standard curve.

2.7. Native polyacrylamide gel electrophoresis

Clear native polyacrylamide gel electrophoresis (nPAGE) was performed to probe the conformers/oligomeric assemblies formed during the aggregation reaction. Twelve percent resolving nPAGE was cast with 4% stacking gel and electrophoresed in 300 mM of Bis–Tris at pH 7.4 as the anode buffer and 300 mM of Bis–Tris, 500 mM tricine at pH 7.4 as the cathode buffer. A constant current of 4 mA was applied while running in the stacking gel and of 6 mA in the resolving gel. The sample for electrophoresis was prepared in 2× sample loading buffer (300 mM of Bis–Tris pH 7.4, 3 M aminocaproic acid, 0.001% Ponceau S). Ten microliter protein samples were drawn fresh from the aggregation reaction and electrophoresed. Electrophoresed gels were stained in Coomassie Brilliant Blue R250 staining solution in acetic acid: methanol: water (1:4:5) for 20 min and destained in acetic acid:methanol:water (1:4:5).

3. Results and discussion

3.1. Thioflavin-T fluorescence assay

A number of *in vitro* studies on amyloidogenic proteins have shown the crucial role of salt concentration on aggregation kinetics. In general, higher salt concentrations lead to faster self-assembly [45,51–54]. This enhanced aggregation rate is attributed to sufficient charge screening at higher salt concentrations thus reducing the repulsive forces among the monomers and facilitating intra and intermolecular interactions governed by hydrophobicity [34,55]. Intramolecular hydrophobic interactions induce partially folded conformations in intrinsically disordered proteins like αSyn, one or more of which could be a nucleation promoting conformation [56]. The possibility of attaining conformations with subtle structural differences in a given solvent condition decisively influences alternative fibril assembly pathways during nucleation, and is proposed to be the basis of heterogeneity [26,57,58]. A recent study on strain like behavior of αSyn amyloids shows formation of fibril (non-periodic) or ribbon (periodic) type of assemblies, highlighting differences in monomer conformations induced by specific reaction conditions [58,59].

With an aim to reduce heterogeneity, we set up fibrillization experiments of A140C αSyn in 10 mM Tris–HCl and 2 mM DTT at pH 7.4 and at low salt concentrations of 1 and 10 mM NaCl, instead of more frequently used concentrations of 50 mM or 100 mM NaCl. Recent reports studying the effect of solvent conditions on αSyn fibrillization clearly demonstrate the tendency of fibrils to form higher order assemblies and floccules at higher NaCl concentrations [32,41]. Such supra-molecular aggregates are not amenable to single fibril level morphological studies by AFM. 0.1 mM EDTA was included in the reactions to enhance the half-life of DTT, which was incorporated to prevent intermolecular disulfide bond formation by the introduced cysteine residue. Inclusion of 0.1 to 1 mM of EDTA has been shown to enhance the stability of thiol additives in protein purification against oxidation by trace metal ions [60]. An experiment to determine the optimal EDTA concentration to maximize half-life of DTT showed 0.1 mM EDTA to be as effective as higher concentrations (data not shown). Thus 0.1 mM EDTA was chosen as the working concentration in EDTA supplemented aggregation reactions.

We observed two clear trends in the ThT curves following fibrillization of A140C mutant in the above-mentioned solvent conditions. Reactions in the presence of 10 mM NaCl showed higher fluorescence intensities compared to those at 1 mM NaCl salt concentration. Also, reactions in the presence of 0.1 mM EDTA reproducibly showed higher fluorescence intensities in the plateau phase of the aggregation reaction as compared to reactions without EDTA (Fig. 1). The measured fluorescence intensities of the reactions with 1 mM NaCl in the presence of EDTA were comparable to those of the reactions with only 10 mM NaCl. In a control experiment, A140C fibrils prepared in 10 mM Tris–HCl, 10 mM NaCl and 2 mM DTT at pH 7.4, were titrated with 0.08 mM to 2.5 mM EDTA at pH 7.4 to examine a possible effect of EDTA on the ThT assay. The results showed no noticeable difference in ThT intensities in the presence/absence of EDTA (data not shown).

An analogous set of experiments with 100 μM wt αSyn in 10 mM Tris–HCl, with 1 or 10 mM NaCl in the absence and presence of 0.1 mM EDTA at pH 7.4 was done to ascertain if the trend observed in A140C is also seen with wt αSyn. Fibrillization reactions in the presence of 0.1 mM EDTA reproducibly showed higher ThT fluorescence values as compared to reactions without EDTA (Fig. S1). Varying the concentration of EDTA from 0.05, 0.1 to 0.2 mM for further optimization of wt aggregations did not show any significant difference in the final fluorescence values (Fig. S2). αSyn aggregation is reported to be a first order

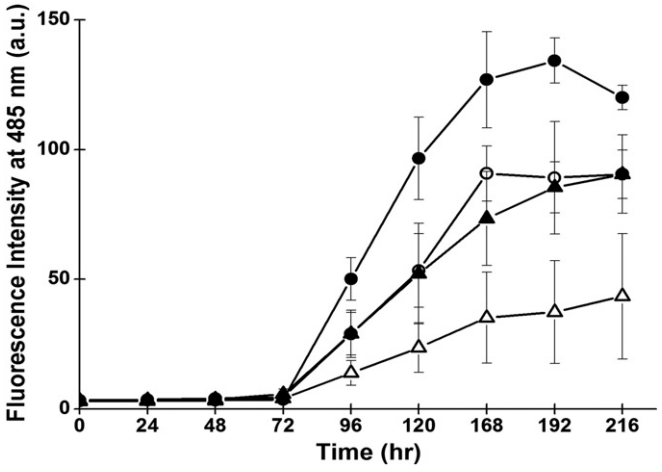

Fig. 1. Kinetics of A140C αSyn aggregation measured by ThT fluorescence as a function of NaCl concentration in the absence or presence of 0.1 mM EDTA. Aggregation buffer included 10 mM Tris–HCl, 2 mM DTT at pH 7.4, and 1 mM NaCl (△, ▲) or 10 mM NaCl (○, ●); without EDTA (open symbols) or with 0.1 mM EDTA (filled symbols). Error bars denote standard deviation among triplicates.

nucleation dependent polymerization reaction [16]. In fibrillization with monomers, primary nucleation is dominant and is characterized by a sigmoidal growth curve in the ThT assay [61]. Higher ThT intensities in the presence of EDTA are thus indicative of more cross-β structure. Determination of residual monomer concentration at the plateau phase of ThT curves showed that reactions with EDTA had lesser monomers left for A140C and wt aggregations (Fig. S3). Together, data from ThT assays and residual monomer concentration analysis suggest that a larger fraction of monomers is incorporated in ThT positive fibrils in the presence of EDTA (Figs. 1, S1 and S3). Lower final fluorescence intensities and higher residual monomer concentrations found for 1 mM NaCl reactions similarly suggest lower cross-β content and less uptake of monomers in fibrils. However, it is also possible that ThT may exhibit differential binding to fibrils prepared under different solvent conditions. Calculation of per μM contribution of fluorescence from each fibril sample using residual monomer concentration and final fluorescence values show that fibrils prepared in the presence of EDTA have 10 to 40% higher fluorescence per μM of protein incorporated into fibrils (Table S1). Thus in solvent conditions with EDTA not only more monomers are included into the fibrils but also the fibrils formed likely bind ThT in a more efficient manner. The same may hold for fibrils formed in 10 mM *versus* 1 mM aggregation conditions.

3.2. AFM imaging and morphology analysis

Fibrils from the end phase of fibrillization reactions (after 192–216 hours) were imaged by AFM using soft tapping mode in air. The fibrils (A140C and wt) were typically several micrometers long, and exhibited distinctive twisted morphology (Figs. S4 and S5) [27]. The key morphological features of twisted amyloid fibrils are their height and periodicity, characteristics that can be experimentally measured with high accuracy using AFM [35,38]. For each solvent condition, around 100 non-overlapping fibrils of at least 1 μm length were quantitatively analyzed for height and periodicity.

The periodicities of A140C fibrils grown in 10 mM NaCl as well as 1 mM NaCl showed a broad distribution, with average periodicities of 99 ± 32 nm and 109 ± 20 nm, respectively. Interestingly, the fibril population produced in 10 mM NaCl appeared to have three distinct groups with average periodicities around 50, 100 and 150 nm (Figs. 2a, b, 3a, and c). However, fibrils grown in the same salt conditions, but in the presence of 0.1 mM EDTA, showed a significantly narrower distribution of periodicities with an average value of 102 ± 6 nm for 10 mM NaCl and 105 ± 6 nm for 1 mM NaCl salt concentrations (Figs. 2c, d, 3b, d and Table 1). Thus, the homogeneity in periodicity of the A140C fibrils appears to be sensitive to the presence of EDTA. In other amyloid forming proteins like β-lactoglobulin [34] and insulin [40] fibril periodicity is reported to vary as a function of fibril height, which is explained by the hierarchical assembly model (HAM), where successive association of protofilaments into protofibrils and fibrils accompanied by mutual twisting gives rise to various periodicities that correlate with measured heights [34,35,37,40,43]. The measured fibril heights in our study, however, were not considerably different for fibrils prepared in 1 or 10 mM NaCl and with or without EDTA. The average heights for fibrils were 6.5 ± 0.7 (1 mM NaCl), 6.3 ± 0.4 (10 mM NaCl), 6.3 ± 0.6 (1 mM NaCl with EDTA) and 6.4 ± 0.4 (10 mM NaCl with EDTA). Also it is noteworthy that fibrils formed in 10 mM NaCl without EDTA and displaying distinct periodicities of 50, 100 and 150 nm did not show differences in height expected for hierarchical assembly (Figs. 2, 3 and Table 1). This observation shows that the morphological parameters of height and periodicity in mature αSyn fibrils formed under the given solvent conditions are not coupled.

A parallel set of experiments probing the effect of inclusion of EDTA on height and periodicity of wt αSyn fibrils was done to assess if the homogeneity in periodicity with EDTA is limited to the A140C mutant or is seen with wt αSyn aggregation as well. Fibrillization was performed using 100 μM wt αSyn in 1 or 10 mM NaCl, with and without 0.1 mM EDTA at pH 7.4. The fibrils formed at 1 mM NaCl showed homogeneous periodicity of 110 ± 10 nm (no EDTA) and 108 ± 7 nm (0.1 mM EDTA). Akin to A140C, at 10 mM NaCl concentration wt αSyn fibril periodicity was more defined in the presence of EDTA with an average value of 107 ± 9 nm as compared to 119 ± 24 nm for fibrils prepared without EDTA (Figs. 4, 5 and Table 1). The height distribution of wt αSyn fibrils formed in the presence of EDTA however showed a slightly narrower distribution when compared to fibrils aggregated without EDTA. It is notable that only reducing the salt concentration from 10 to 1 mM NaCl, in the absence of EDTA, makes the aggregations more homogeneous regarding morphology of the fibrils formed. The kinetics of fibrillization are however slower, and a smaller protein fraction is included in fibrils indicating that very low salt conditions are less efficient conditions for fibrillization.

3.3. DTNB assay

All fibrillization reactions with the A140C mutant included DTT as a reducing agent in order to inhibit intermolecular disulfide bond formation through the cysteine residue at position 140. Formation of cysteine dimers is a favored reaction, such that the protein aliquots thawed from −80 °C often showed dimer protein bands on native gels (Fig. S6). A typical aggregation reaction starting with monomers, as probed by ThT fluorescence, takes on average 7 days to reach the plateau, while DTT has a much shorter half-life. The half-life of DTT has been previously shown to be affected by the presence of free divalent metal ions which enhance its oxidation [62]. Thus, in order to prevent oxidation of DTT by trace metal ions, 0.1 mM EDTA was included in the aggregation reactions. The effect of EDTA on the half-life of DTT was probed by quantitating free thiols in the aggregation reaction by a DTNB assay. In the DTNB assay, DTNB [5,5′-dithiobis-(2-nitrobenzoic acid)] reacts with free thiols in a 1:1 stoichiometric ratio in aqueous solvents, forming 2-nitro-5-thiobenzoate (NTB^{2-})

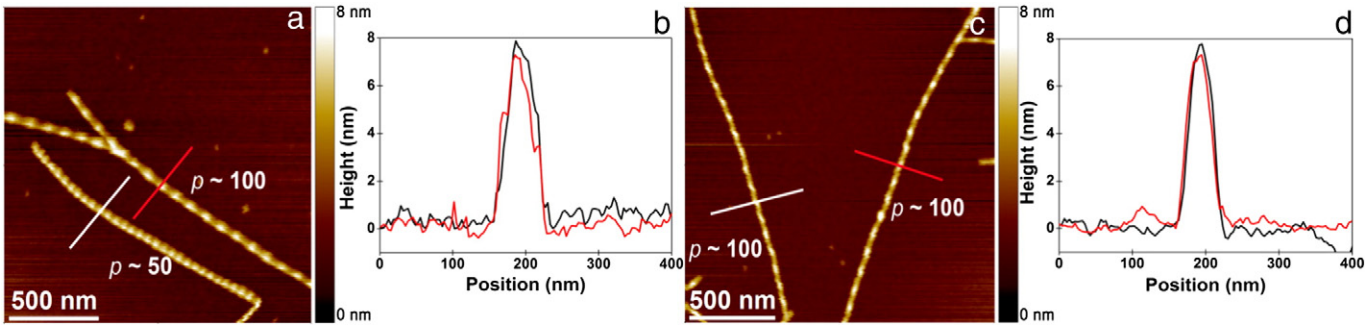

Fig. 2. Representative AFM height images of A140C αSyn (a, c) and corresponding height profiles (b, d). Tapping mode AFM height images of A140C αSyn fibrils prepared in 10 mM Tris–HCl, 10 mM NaCl, 2 mM DTT at pH 7.4 and in the absence (a) or presence (c) of 0.1 mM EDTA. White and red lines in (a) and (c) indicate positions of line profiles depicted in (b) and (d). Labels (50, 100) signify approximate value for periodicity (p) of the fibrils in nm. AFM image size: 1.7 × 1.7 μm.

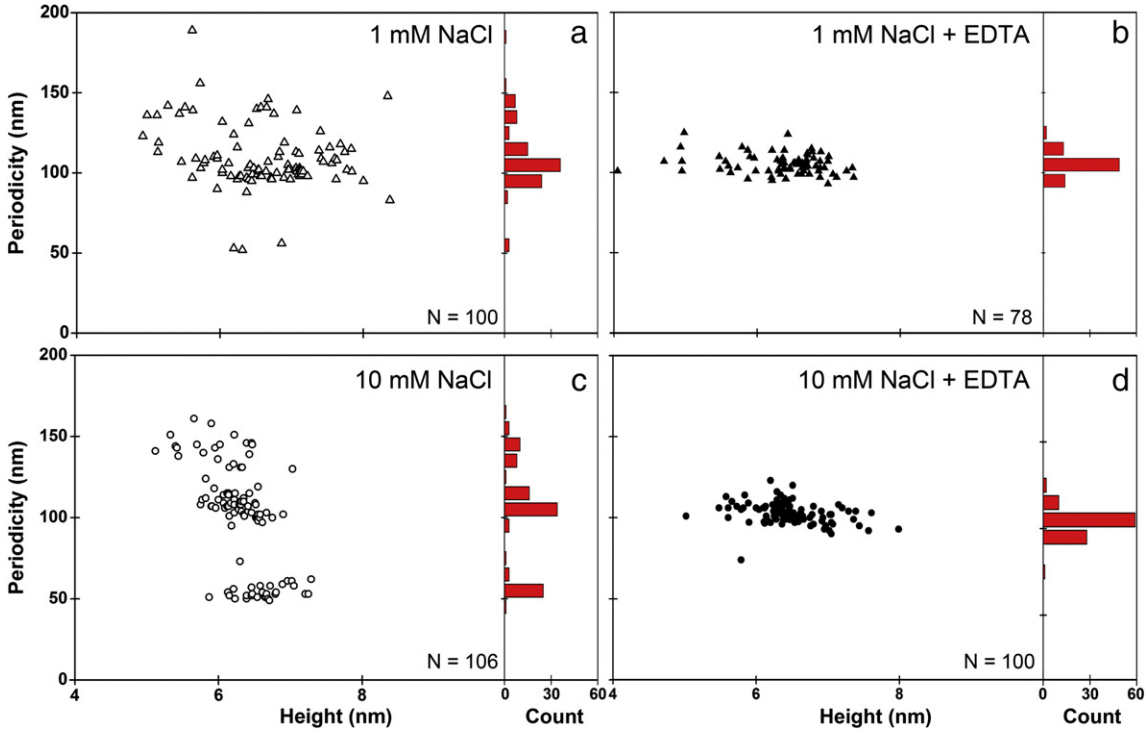

Fig. 3. Scatter plots representing quantitative morphological features of A140C αSyn fibrils prepared in 10 mM Tris–HCl, 2 mM DTT at pH 7.4 with 1 mM NaCl (△,▲) or 10 mM NaCl (○,●) in the absence (a, c — open symbols) or presence (b, d — filled symbols) of 0.1 mM EDTA. Next to each scatter plot a histogram in red shows the distribution of periodicities for the fibrils. Bin size: 10 nm. (a, c) Fibrils grown in the absence of EDTA display a broad distribution of periodicities; notably aggregations in 10 mM NaCl result in three fibril groups with average periodicities around 50, 100 and 150 nm. (b, d) Fibrils produced in the presence of EDTA show one dominant population corresponding to an average periodicity of about 100 nm. Fibril periodicities show no apparent correlation with heights in the absence (a, c) or presence (b, d) of EDTA.

which is intense yellow in color and can be quantified by absorbance at 412 nm [63]. In reactions without EDTA the half-life of DTT was about 1 day whereas in the presence of 0.1 mM EDTA the half-life increased significantly to more than 9 days (Fig. S7). A control experiment to check if presence of EDTA alone could bring about the colorimetric change in the DTNB assay showed negative results (data not shown). In the presence of EDTA, the notable increase in the half-life of DTT as well as the qualitative influence on fibrillization of αSyn is suggestive of two distinct possibilities. EDTA primarily acts as a chelating agent and sequesters the trace divalent metal ions; as a result it prevents oxidation of DTT in A140C fibrillization. Additionally this chelating property possibly curbs interaction of metal ions with the negatively charged C-terminus of αSyn monomers, thereby altering its conformation to one favorable for aggregation [52,64]. Previous studies have shown that sequestration of metal ions by specific chelators leads to formation of more ordered fibrils, which have a sharper X-ray diffraction pattern owing to better alignment of the sample [65]. Evidence for enhancement of half-life of DTT and modulation of metal ion interaction with αSyn monomer being independent of each other is apparent in fibrillization of wt αSyn in the presence of EDTA but without DTT, where similar ThT kinetics (Fig. S1) and homogeneity in morphology was observed (Fig. 5). Also experiments including DTT in aggregation conditions to probe the effect of reducing conditions on wt aggregation did not show any decisive trend in the ThT assay (Fig. S8).

3.4. Native PAGE analysis

Native polyacrylamide gel electrophoresis (nPAGE) is sensitive to the conformations of protein molecules and can be insightful about aggregation events. A140C aggregation at different NaCl concentrations, with and without EDTA, was followed on 12% nPAGE for qualitative analysis of conformers and oligomeric assemblies. Initially, all the fractions exhibited a similar profile, but by 72 hours, concomitant with near depletion of DTT in reactions without EDTA, additional faster migrating bands (below the monomer band) were apparent together with a dimer band. However, in reactions with EDTA no additional bands could be observed, and over time, monomer bands became fainter indicating exhaustion of the free monomers in the solution (Figs. 6 and S6). The formation of additional faster migrating αSyn conformers and dimers appears to be prevented by DTT (half-life of which is critically influenced by EDTA) as they tend to appear only once DTT is exhausted in the solution. We also performed an aggregation with TCEP as the reducing agent using 100 μM A140C αSyn in 10 mM Tris–HCl, 10 mM NaCl, 2 mM TCEP at pH 7.4. TCEP is a stronger and a more stable reducing agent than DTT and does not require EDTA.

Table 1
Summary of average height and periodicity measurement of A140C and wt αSyn fibrils (±stdv). Number of fibrils analyzed for each solvent condition is shown in parentheses.

0.1 mM EDTA	A140C		wt		Morphological observables
	1 mM NaCl	10 mM NaCl	1 mM NaCl	10 mM NaCl	
-	6.5 ± 0.7 (100)	6.3 ± 0.4 (106)	6.7 ± 0.4 (104)	6.1 ± 0.7 (100)	Height (h) (nm)
+	6.3 ± 0.6 (78)	6.4 ± 0.4 (100)	6.7 ± 0.5 (100)	6.9 ± 0.6 (105)	
-	109 ± 20 (100)	99 ± 32 (106)	110 ± 10 (104)	119 ± 24 (100)	Periodicity (p) (nm)
+	105 ± 6 (78)	102 ± 6 (100)	108 ± 7 (100)	107 ± 9 (105)	

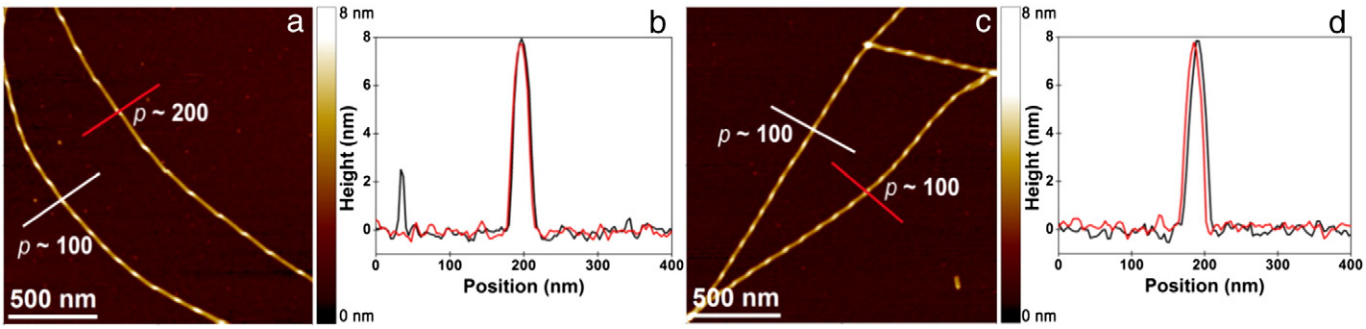

Fig. 4. Representative AFM height images of wt αSyn (a, c) and corresponding height profiles (b, d). Tapping mode AFM height images of wt αSyn fibrils prepared in 10 mM Tris–HCl, 10 mM NaCl at pH 7.4 and in the absence (a) or presence (c) of 0.1 mM EDTA. White and red lines in (a) and (c) indicate positions of the line profiles depicted in (b) and (d). Labels (100, 200) signify approximate values for periodicity (p) of the fibrils in nm. AFM image size: 1.7 × 1.7 μm.

Fibrillization in the presence of TCEP showed faster aggregation kinetics in the ThT assay than reactions with DTT (±0.1 mM EDTA) (Fig. S9). Also on nPAGE no additional bands were observed after 72 hours of aggregation, thus confirming that stable reducing conditions inhibit their formation (Fig. S10).

In wt fibrillization reactions (no DTT) followed on nPAGE similar to A140C, a discernible difference in the monomer band intensity between reactions with and without EDTA could be seen at 72 hours and later. Also in the presence of EDTA no additional bands could be observed (Fig. S11). Together these results, in agreement with ThT and RMC analyses, demonstrate that a higher fraction of monomers is incorporated into wt and A10C fibrils in reactions with EDTA.

4. Conclusions

In this work we show that fibrillization of αSyn can be carefully modulated by solution conditions to produce morphologically homogeneous populations of fibrils. The fibrils were prepared in low salt conditions in an effort to reduce stochasticity inherent with amyloid systems. Buffer conditions of 10 mM Tris–HCl, 10 mM NaCl, 2 mM DTT and 0.1 mM EDTA at pH 7.4 yielded A140C αSyn fibrils displaying a narrow distribution of periodicities with an average value of 102 ± 6 nm; in similar solvent conditions but without DTT, wt αSyn formed fibrils with an average periodicity of 107 ± 9 nm. Inclusion of EDTA is instrumental in forming fibrils with well-defined periodicity, by two likely effects involving its chelating function. Firstly, in reactions with thiol containing A140C αSyn, it reduces oxidation of DTT by metal ions, significantly enhancing DTT's half-life and thus preventing protein dimerization. Secondly, it prevents the interaction of metal ions with the negatively charged C-terminus of αSyn monomers potentially introducing a conformational bias which may positively influence the nucleation. Morphological analyses by AFM evidently demonstrate the formation of homogeneous fibrils with EDTA. Additionally, ThT assays, RMC and nPAGE results support the proposition of more efficient incorporation of αSyn monomers into fibrils in the presence of 0.1 mM EDTA. The present results are an important step forward for

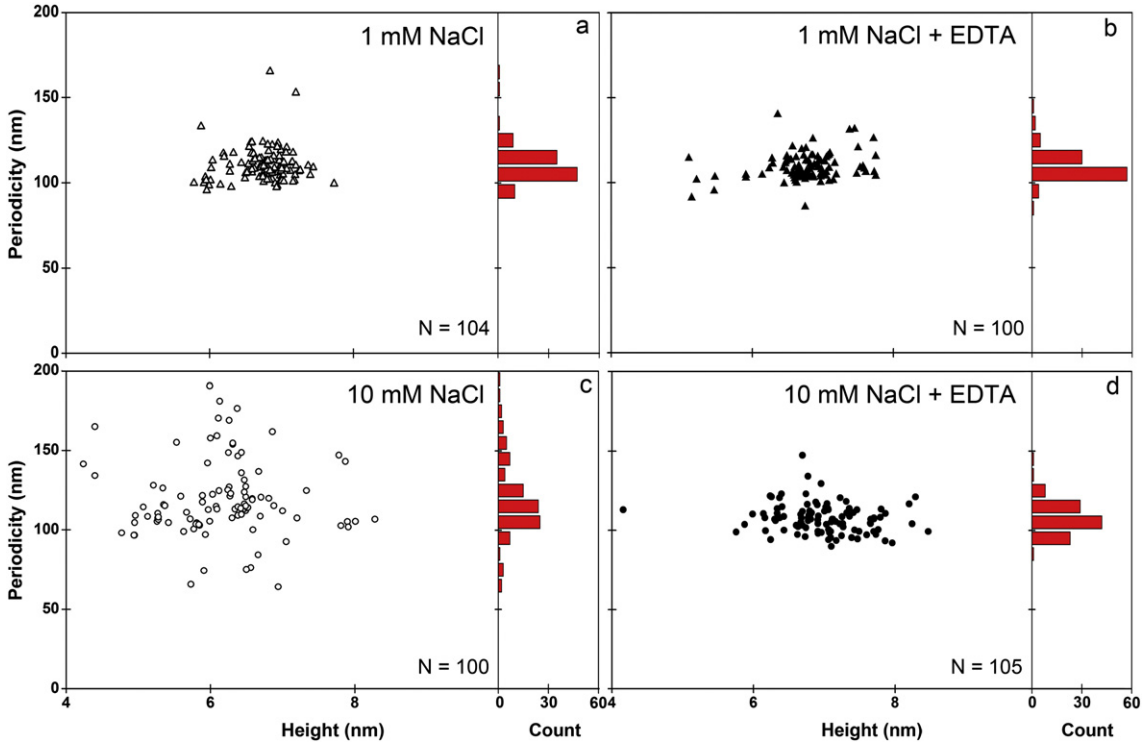

Fig. 5. Scatter plots representing quantitative morphological features of wt αSyn fibrils prepared in 10 mM Tris–HCl at pH 7.4 with 1 mM NaCl (△,▲) or 10 mM NaCl (○,●) in the absence (a, c — open symbols) or presence (b, d — filled symbols) of 0.1 mM EDTA. Next to each scatter plot a histogram in red shows the distribution of periodicities for the fibrils. Bin size: 10 nm. (a, c) Fibrils grown in the absence of EDTA display a broad distribution of fibril periodicities notably for reactions aggregated at 10 mM NaCl. (b, d) Fibrils produced in the presence of EDTA show a narrow distribution of fibril periodicities. Fibril periodicities show no apparent correlation with heights in the absence (a, c) or presence (b, d) of EDTA.

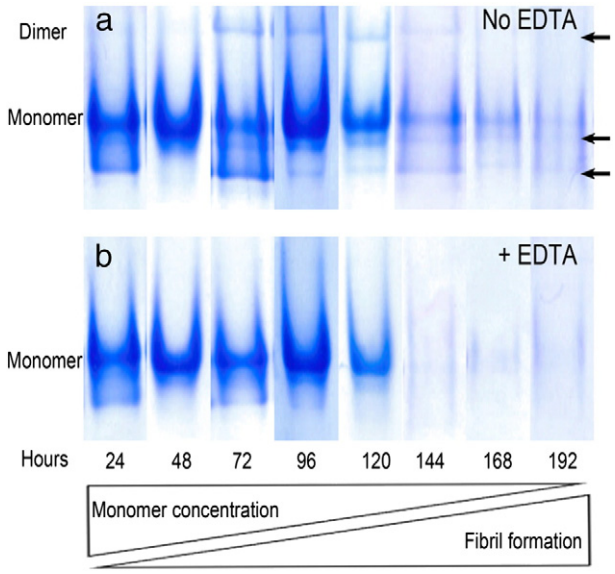

Fig. 6. Twelve percent clear native PAGE analysis of A140C αSyn fibrillization reactions. Aggregation reactions were set up in 10 mM Tris–HCl, 10 mM NaCl, 2 mM DTT at pH 7.4 and in the absence (a) or presence (b) of 0.1 mM EDTA. Lanes in panel (a) and (b) show qualitative differences in the active aggregation reactions as a function of time. Note the appearance of additional bands in the fractions without EDTA at 72 hours and later (indicated by black arrows). Monomer protein concentration decreases with time dependent accumulation of fibrillar species, which do not electrophorese in the polyacrylamide gel. Lanes in panel (a) and (b) are parts of separate gels electrophoresed for each time point. For complete gels refer to Fig. S6.

using amyloids as bio-nanomaterials as it provides a practical handle to prepare homogeneous and reproducible amyloid fibrils.

Acknowledgements

We thank Kirsten van Leijenhorst-Groener, Yvonne Kraan and Nathalie Schilderink for protein expression and purification, and Dr. Martin Bennink, Kees van der Werf and Robert Molenaar for advice on AFM. This work is supported by NanoNextNL, a micro and nanotechnology consortium of the Government of The Netherlands and 130 partners. We also acknowledge support from the Foundation for Fundamental Research on Matter (FOM), which is part of the Netherlands Organization for Scientific Research (NWO).

Appendix A. Supplementary data

Supplementary data to this article can be found online at http://dx.doi.org/10.1016/j.bbapap.2014.09.007.

References

[1] M.G. Spillantini, M.L. Schmidt, V.M. Lee, J.Q. Trojanowski, R. Jakes, M. Goedert, Alpha-synuclein in Lewy bodies, Nature 388 (1997) 839–840.
[2] L. Stefanis, alpha-Synuclein in Parkinson's disease, Cold Spring Harb. Perspect. Med. 2 (2012) a009399, (Epub ahead of print).
[3] F. Chiti, C.M. Dobson, Protein misfolding, functional amyloid, and human disease, Annu. Rev. Biochem. 75 (2006) 333–366.
[4] A.F. Teich, M. Patel, O. Arancio, A reliable way to detect endogenous murine beta-amyloid, PLoS One 8 (2013) e55647, (Epub ahead of print).
[5] M. Ono, H. Saji, SPECT imaging agents for detecting cerebral beta-amyloid plaques, Int. J. Mol. Imaging 2011 (2011) 543267, (Epub ahead of print).
[6] J. Bieschke, J. Russ, R.P. Friedrich, D.E. Ehrnhoefer, H. Wobst, K. Neugebauer, E.E. Wanker, EGCG remodels mature alpha-synuclein and amyloid-beta fibrils and reduces cellular toxicity, Proc. Natl. Acad. Sci. U. S. A. 107 (2010) 7710–7715.
[7] J.H. Lu, M.T. Ardah, S.S. Durairajan, L.F. Liu, L.X. Xie, W.F. Fong, M.Y. Hasan, J.D. Huang, O.M. El-Agnaf, M. Li, Baicalein inhibits formation of alpha-synuclein oligomers within living cells and prevents Abeta peptide fibrillation and oligomerisation, Chembiochem 12 (2011) 615–624.
[8] M.S. Wang, S. Boddapati, S. Emadi, M.R. Sierks, Curcumin reduces alpha-synuclein induced cytotoxicity in Parkinson's disease cell model, BMC Neurosci. 11 (2010) 57.
[9] D. Hamada, I. Yanagihara, K. Tsumoto, Engineering amyloidogenicity towards the development of nanofibrillar materials, Trends Biotechnol. 22 (2004) 93–97.
[10] S. Mankar, A. Anoop, S. Sen, S.K. Maji, Nanomaterials: amyloids reflect their brighter side, Nano Rev. 2 (2011).
[11] C.L. Chen, N.L. Rosi, Peptide-based methods for the preparation of nanostructured inorganic materials, Angew. Chem. Int. Ed. Engl. 49 (2010) 1924–1942.
[12] E. Gazit, Use of biomolecular templates for the fabrication of metal nanowires, FEBS J. 274 (2007) 317–322.
[13] R. Colby, J. Hulleman, S. Padalkar, J.C. Rochet, L.A. Stanciu, Biotemplated synthesis of metallic nanoparticle chains on an alpha-synuclein fiber scaffold, J. Nanosci. Nanotechnol. 8 (2008) 973–978.
[14] T. Scheibel, R. Parthasarathy, G. Sawicki, X.M. Lin, H. Jaeger, S.L. Lindquist, Conducting nanowires built by controlled self-assembly of amyloid fibers and selective metal deposition, Proc. Natl. Acad. Sci. U. S. A. 100 (2003) 4527–4532.
[15] A. Herland, P. Bjork, K.P.R. Nilsson, J.D.M. Olsson, P. Asberg, P. Konradsson, P. Hammarstrom, O. Inganas, Electroactive luminescent self-assembled bio-organic nanowires: integration of semiconducting oligoelectrolytes within amyloidogenic proteins, Adv. Mater. 17 (2005) 1466–1471.
[16] S.J. Wood, J. Wypych, S. Steavenson, J.C. Louis, M. Citron, A.L. Biere, alpha-Synuclein fibrillogenesis is nucleation-dependent. Implications for the pathogenesis of Parkinson's disease, J. Biol. Chem. 274 (1999) 19509–19512.
[17] J.T. Jarrett, P.T. Lansbury Jr., Seeding "one-dimensional crystallization" of amyloid: a pathogenic mechanism in Alzheimer's disease and scrapie? Cell 73 (1993) 1055–1058.
[18] S.I. Cohen, S. Linse, L.M. Luheshi, E. Hellstrand, D.A. White, L. Rajah, D.E. Otzen, M. Vendruscolo, C.M. Dobson, T.P. Knowles, Proliferation of amyloid-beta42 aggregates occurs through a secondary nucleation mechanism, Proc. Natl. Acad. Sci. U. S. A. 110 (2013) 9758–9763.
[19] V. Fodera, F. Librizzi, M. Groenning, M. van de Weert, M. Leone, Secondary nucleation and accessible surface in insulin amyloid fibril formation, J. Phys. Chem. B 112 (2008) 3853–3858.
[20] T.P. Knowles, C.A. Waudby, G.L. Devlin, S.I. Cohen, A. Aguzzi, M. Vendruscolo, E.M. Terentjev, M.E. Welland, C.M. Dobson, An analytical solution to the kinetics of breakable filament assembly, Science 326 (2009) 1533–1537.
[21] H. Heise, W. Hoyer, S. Becker, O.C. Andronesi, D. Riedel, M. Baldus, Molecular-level secondary structure, polymorphism, and dynamics of full-length alpha-synuclein fibrils studied by solid-state NMR, Proc. Natl. Acad. Sci. U. S. A. 102 (2005) 15871–15876.
[22] W.S. Gosal, I.J. Morten, E.W. Hewitt, D.A. Smith, N.H. Thomson, S.E. Radford, Competing pathways determine fibril morphology in the self-assembly of beta2-microglobulin into amyloid, J. Mol. Biol. 351 (2005) 850–864.
[23] M. Fandrich, J. Meinhardt, N. Grigorieff, Structural polymorphism of Alzheimer Abeta and other amyloid fibrils, Prion 3 (2009) 89–93.
[24] R. Kodali, R. Wetzel, Polymorphism in the intermediates and products of amyloid assembly, Curr. Opin. Struct. Biol. 17 (2007) 48–57.
[25] I. Usov, J. Adamcik, R. Mezzenga, Polymorphism complexity and handedness inversion in serum albumin amyloid fibrils, ACS Nano 7 (2013) 10465–10474.
[26] C. Goldsbury, P. Frey, V. Olivieri, U. Aebi, S.A. Muller, Multiple assembly pathways underlie amyloid-beta fibril polymorphisms, J. Mol. Biol. 352 (2005) 282–298.
[27] M.E. van Raaij, I.M. Segers-Nolten, V. Subramaniam, Quantitative morphological analysis reveals ultrastructural diversity of amyloid fibrils from alpha-synuclein mutants, Biophys. J. 91 (2006) L96–L98.
[28] M. Vilar, H.T. Chou, T. Luhrs, S.K. Maji, D. Riek-Loher, R. Verel, G. Manning, H. Stahlberg, R. Riek, The fold of alpha-synuclein fibrils, Proc. Natl. Acad. Sci. U. S. A. 105 (2008) 8637–8642.
[29] C. Ionescu-Zanetti, R. Khurana, J.R. Gillespie, J.S. Petrick, L.C. Trabachino, L.J. Minert, S. A. Carter, A.L. Fink, Monitoring the assembly of Ig light-chain amyloid fibrils by atomic force microscopy, Proc. Natl. Acad. Sci. U. S. A. 96 (1999) 13175–13179.
[30] C. Lara, S. Gourdin-Bertin, J. Adamcik, S. Bolisetty, R. Mezzenga, Self-assembly of ovalbumin into amyloid and non-amyloid fibrils, Biomacromolecules 13 (2012) 4213–4221.
[31] C. Lara, J. Adamcik, S. Jordens, R. Mezzenga, General self-assembly mechanism converting hydrolyzed globular proteins into giant multistranded amyloid ribbons, Biomacromolecules 12 (2011) 1868–1875.
[32] A.K. Buell, C. Galvagnion, R. Gaspar, E. Sparr, M. Vendruscolo, T.P. Knowles, S. Linse, C.M. Dobson, Solution conditions determine the relative importance of nucleation and growth processes in alpha-synuclein aggregation, Proc. Natl. Acad. Sci. U. S. A. 111 (2014) 7671–7676.
[33] J. Pronchik, X. He, J.T. Giurleo, D.S. Talaga, In vitro formation of amyloid from alpha-synuclein is dominated by reactions at hydrophobic interfaces, J. Am. Chem. Soc. 132 (2010) 9797–9803.
[34] J. Adamcik, R. Mezzenga, Adjustable twisting periodic pitch of amyloid fibrils, Soft Matter 7 (2011) 5437–5443.
[35] R. Khurana, C. Ionescu-Zanetti, M. Pope, J. Li, L. Nielson, M. Ramirez-Alvarado, L. Regan, A.L. Fink, S.A. Carter, A general model for amyloid fibril assembly based on morphological studies using atomic force microscopy, Biophys. J. 85 (2003) 1135–1144.
[36] M.E. van Raaij, J. van Gestel, I.M. Segers-Nolten, S.W. de Leeuw, V. Subramaniam, Concentration dependence of alpha-synuclein fibril length assessed by quantitative atomic force microscopy and statistical-mechanical theory, Biophys. J. 95 (2008) 4871–4878.
[37] J.D. Harper, S.S. Wong, C.M. Lieber, P.T. Lansbury Jr., Assembly of A beta amyloid protofibrils: an in vitro model for a possible early event in Alzheimer's disease, Biochemistry 38 (1999) 8972–8980.
[38] J. Adamcik, J.M. Jung, J. Flakowski, P. De Los Rios, G. Dietler, R. Mezzenga, Understanding amyloid aggregation by statistical analysis of atomic force microscopy images, Nat. Nanotechnol. 5 (2010) 423–428.

[39] W.F. Xue, A.L. Hellewell, W.S. Gosal, S.W. Homans, E.W. Hewitt, S.E. Radford, Fibril fragmentation enhances amyloid cytotoxicity, J. Biol. Chem. 284 (2009) 34272–34282.
[40] J.L. Jimenez, E.J. Nettleton, M. Bouchard, C.V. Robinson, C.M. Dobson, H.R. Saibil, The protofilament structure of insulin amyloid fibrils, Proc. Natl. Acad. Sci. U. S. A. 99 (2002) 9196–9201.
[41] S.A. Semerdzhiev, D.R. Dekker, V. Subramaniam, M.M. Claessens, Self-assembly of protein fibrils into suprafibrillar aggregates: bridging the nano- and mesoscale, ACS Nano 8 (2014) 5543–5551.
[42] S. Campioni, G. Carret, S. Jordens, L. Nicoud, R. Mezzenga, R. Riek, The presence of an air–water interface affects formation and elongation of alpha-synuclein fibrils, J. Am. Chem. Soc. 136 (2014) 2866–2875.
[43] Z. Qin, D. Hu, S. Han, D.P. Hong, A.L. Fink, Role of different regions of alpha-synuclein in the assembly of fibrils, Biochemistry 46 (2007) 13322–13330.
[44] W.F. Xue, S.W. Homans, S.E. Radford, Amyloid fibril length distribution quantified by atomic force microscopy single-particle image analysis, Protein Eng. Des. Sel. 22 (2009) 489–496.
[45] W. Hoyer, T. Antony, D. Cherny, G. Heim, T.M. Jovin, V. Subramaniam, Dependence of alpha-synuclein aggregate morphology on solution conditions, J. Mol. Biol. 322 (2002) 383–393.
[46] L. Giehm, N. Lorenzen, D.E. Otzen, Assays for alpha-synuclein aggregation, Methods 53 (2011) 295–305.
[47] M.E. Herva, S. Zibaee, G. Fraser, R.A. Barker, M. Goedert, M.G. Spillantini, Anti-amyloid compounds inhibit alpha-synuclein aggregation induced by Protein Misfolding Cyclic Amplification (PMCA), J. Biol. Chem. 289 (2014) 11897–11905.
[48] C. Del Mar, E.A. Greenbaum, L. Mayne, S.W. Englander, V.L. Woods Jr., Structure and properties of alpha-synuclein and other amyloids determined at the amino acid level, Proc. Natl. Acad. Sci. U. S. A. 102 (2005) 15477–15482.
[49] T. Guilliams, F. El-Turk, A.K. Buell, E.M. O'Day, F.A. Aprile, E.K. Esbjorner, M. Vendruscolo, N. Cremades, E. Pardon, L. Wyns, M.E. Welland, J. Steyaert, J. Christodoulou, C.M. Dobson, E. De Genst, Nanobodies raised against monomeric alpha-synuclein distinguish between fibrils at different maturation stages, J. Mol. Biol. 425 (2013) 2397–2411.
[50] G.R. Grimsley, C.N. Pace, Spectrophotometric determination of protein concentration, Current Protocols in, Protein Science, vol. 33, 2004, pp. 3.1.1–3.1.9.
[51] S. Fujiwara, F. Matsumoto, Y. Yonezawa, Effects of salt concentration on association of the amyloid protofilaments of hen egg white lysozyme studied by time-resolved neutron scattering, J. Mol. Biol. 331 (2003) 21–28.
[52] W. Hoyer, D. Cherny, V. Subramaniam, T.M. Jovin, Impact of the acidic C-terminal region comprising amino acids 109-140 on alpha-synuclein aggregation in vitro, Biochemistry 43 (2004) 16233–16242.
[53] P.J. Marek, V. Patsalo, D.F. Green, D.P. Raleigh, Ionic strength effects on amyloid formation by amylin are a complicated interplay among Debye screening, ion selectivity, and Hofmeister effects, Biochemistry 51 (2012) 8478–8490.
[54] A.K. Buell, P. Hung, X. Salvatella, M.E. Welland, C.M. Dobson, T.P. Knowles, Electrostatic effects in filamentous protein aggregation, Biophys. J. 104 (2013) 1116–1126.
[55] B. Raman, E. Chatani, M. Kihara, T. Ban, M. Sakai, K. Hasegawa, H. Naiki, M. Rao Ch, Y. Goto, Critical balance of electrostatic and hydrophobic interactions is required for beta 2-microglobulin amyloid fibril growth and stability, Biochemistry 44 (2005) 1288–1299.
[56] V.N. Uversky, J. Li, A.L. Fink, Evidence for a partially folded intermediate in alpha-synuclein fibril formation, J. Biol. Chem. 276 (2001) 10737–10744.
[57] A.T. Petkova, R.D. Leapman, Z. Guo, W.M. Yau, M.P. Mattson, R. Tycko, Self-propagating, molecular-level polymorphism in Alzheimer's beta-amyloid fibrils, Science 307 (2005) 262–265.
[58] L. Bousset, L. Pieri, G. Ruiz-Arlandis, J. Gath, P.H. Jensen, B. Habenstein, K. Madiona, V. Olieric, A. Bockmann, B.H. Meier, R. Melki, Structural and functional characterization of two alpha-synuclein strains, Nat. Commun. 4 (2013) 2575.
[59] J. Gath, L. Bousset, B. Habenstein, R. Melki, A. Bockmann, B.H. Meier, Unlike twins: an NMR comparison of two alpha-synuclein polymorphs featuring different toxicity, PLoS One 9 (2014) e90659, (Epub ahead of print).
[60] R. Stevens, L. Stevens, N.C. Price, The stabilities of various thiol compounds used in protein purifications, Biochem. Educ. 11 (1983).
[61] S.I. Cohen, M. Vendruscolo, C.M. Dobson, T.P. Knowles, From macroscopic measurements to microscopic mechanisms of protein aggregation, J. Mol. Biol. 421 (2012) 160–171.
[62] J.G. Charrier, C. Anastasio, On dithiothreitol (DTT) as a measure of oxidative potential for ambient particles: evidence for the importance of soluble transition metals, Atmos. Chem. Phys. 12 (2012) 11317–11350.
[63] C.K. Riener, G. Kada, H.J. Gruber, Quick measurement of protein sulfhydryls with Ellman's reagent and with 4,4'-dithiodipyridine, Anal. Bioanal. Chem. 373 (2002) 266–276.
[64] V.N. Uversky, J. Li, A.L. Fink, Metal-triggered structural transformations, aggregation, and fibrillation of human alpha-synuclein. A possible molecular NK between Parkinson's disease and heavy metal exposure, J. Biol. Chem. 276 (2001) 44284–44296.
[65] B. Liu, A. Moloney, S. Meehan, K. Morris, S.E. Thomas, L.C. Serpell, R. Hider, S.J. Marciniak, D.A. Lomas, D.C. Crowther, Iron promotes the toxicity of amyloid beta peptide by impeding its ordered aggregation, J. Biol. Chem. 286 (2011) 4248–4256.